Nihal H. Jabr [1]
Ahmed K. Abbas [1]
Isam M. Ibrahim [2]

[1] *Department of Physics, College of Science, University of Wasit, Wasit, IRAQ*
[2] *Department of Physics, College of Science, University of Baghdad, Baghdad, IRAQ*

Effects of Energy and Wavelength on Laser-Induced Breakdown Spectroscopy of Ablated Tantalum Plasma

In this study, the characteristics of plasma such as electron temperature, electron density, plasma frequency, Debye length, and Debye number have been investigated by the laser-induced breakdown spectroscopy (LIBS) of tantalum (Ta) plasma generated by different laser energies. It was observed that the electron temperature of Ta plasma is ranging from 1.26 to 2.29 eV using 532nm laser wavelength and from 0.57 to 2.93 eV using 1064nm laser wavelength. In a similar manner, electron density was observed to be in the range of 1.90×10^{18}–2.25×10^{18} cm^{-3} using 532nm and in the range of 0.71×10^{18}–1.13×10^{18} cm^{-3} using 1064nm. This study includes the evaluation of optical properties of Ta plasma via UV-visible spectroscopy within the 190–1100nm range. Furthermore, the study explores the crystalline structure and zeta-potential values of 22.55mV using 1064nm and 24.17mV using 532nm, highlighting their roles in understanding material ablation and plasma dynamics under different laser conditions.

Keywords: Laser ablation; Zeta potential; Electron temperature; Electron density
Received: 22 May 2024; Revised: 13 July 2024; Accepted: 20 July 2024

1. Introduction

Basically, laser ablation of materials is the removal of material from a solid surface by a high-intensity laser beam [1]. The interaction of the laser with the target material causes rapid heating, melting, and vaporization of material at the surface, hence forming a plasma plume [2]. This plasma plume includes a mixture of ionized species, neutral atoms, and molecules [3]. The role that laser parameters, such as energy and wavelength, play in forming plasma properties for applications like material processing, various kinds of analytical techniques, and elementary studies of the physics of plasma has been a point of interest lately [4-11]. Tantalum belongs to a category of refractory metals with an appreciably high melting point, excellent corrosion resistance, and good electrical conductivity [12-16]. Plasma temperature can be estimated using various methods, one of which is the Boltzmann plot method. The Boltzmann equation is given by [17-20]:

$$\ln\left(\frac{I_{ji}\lambda_{ji}}{g_{ji}A_{ji}}\right) = \left(\frac{E_j}{k_B T_e}\right) + \left(\frac{N(T)}{U(T)}\right) \quad (1)$$

The parameters λ_{ji}, I_{ji}, g_{ji}, and A_{ji} represent the wavelength, intensity, statistical weight, and transition probability associated with transitions between upper level state (j) and lower level state (i), respectively [21-23], and k_B is Boltzmann's constant

Electron density can be estimated using the Stark broadening of spectral lines. The Stark broadening equation is given by [24]:

$$n_e(cm^{-3}) = \left[\frac{\Delta\lambda}{2\omega_s}\right] N_r \quad (2)$$

where $\Delta\lambda$ is the full-width at half maximum (FWHM) of the line, and ω_s is the theoretical line full-width Stark broadening parameter calculated at the same reference electron density $N_r=10^{16}$ cm^{-3} [25-27].

The plasma frequency can be given as:

$$\omega_{pe} = \sqrt{\frac{n_e e^2}{m_e \varepsilon_0}} \quad (3)$$

where ε_0 is the permittivity of free space, m_e is the mass of the electron and e is the charge of an electron. Debye's length can be calculated by the formula [28]:

$$\lambda_D = \sqrt{\frac{\varepsilon_0 k_B T_e}{e^2 n_e}} \quad (4)$$

The number of particles within the Debye sphere (N_D) is an important parameter and is given by [29]:

$$N_D = n_e\left[\frac{4\pi\lambda_D^3}{3}\right] \quad (5)$$

The primary aim of this work is to systematically investigate and understand the impact of varying laser energies and wavelengths on the plasma properties generated from the ablation of tantalum (Ta).

2. Experimental Part

In this respect, 99.99% pure tantalum metal was used in this work to study the influence of Laser ablation under different conditions. The Tantalum samples were bombarded by a pulsed Nd:YAG laser. This laser system was operated at an indefinite frequency of 6 Hz with two different wavelengths, 1064 nm and 532nm, to understand the concepts of wavelength on the ablation process. In addition, energies of the laser show a big range from 200 to 800mJ; hence, this will be one in-depth study about the effect of laser energy on ablation characteristics. The light emitted from the plasma plume was collected and routed to a THORLABS CCS200 spectroscope. This spectroscope is used within a wavelength window of 200-1000nm, making it compatible with taking an emission spectra of different species in plasma. With a spectral resolution better than 0.5 nm full width at half maximum at 633nm, it provided measurements with an accuracy required for detailed analysis. The role of the optical fiber in this experimental setup was playing a crucial role since it transmitted the collected light into the entrance slit of the spectrometer. The optical fiber fronts the axis of the laser beam at an angle of about 45°, ensuring that most of the light will be transmitted with less menace of splashing or appreciable disturbance of the plasma jet.

3. Results and Discussion

Figures (1) and (2) represent the emission spectra at the surface of tantalum (Ta), recorded using a laser pulse energy varied from 200 to 800 mJ in distilled water. The laser was running at 1064nm and 532nm, producing different spectral responses with changing excitation conditions. The major factors contributing to increased spectrum intensity with increased laser energy include increased ablation, excitation of atoms and ions, electron and ion densities in the plasma, plasma temperature, and better energy transfer from the laser to the tantalum surface. These are some of the major parameters that contribute to increased emission of light, hence higher spectral intensity in the registered spectra. Table (1) summarizes the strain, inter-planar spacing and crystalline size of Ta nanoparticles (NPs).

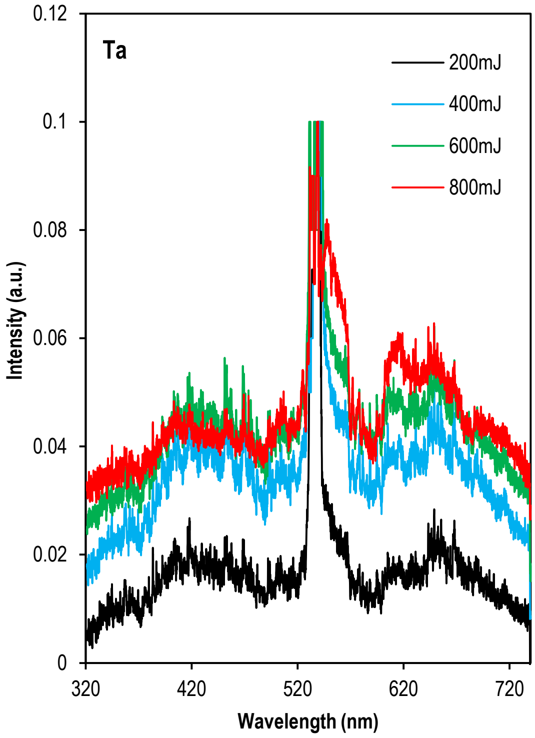

Fig. (1) Emission spectra of Ta target in distilled water produced using 1064nm laser and different laser energies

Figure (3) is the XRD pattern of quartzite phase rutile Ta NPs. The identification of the phase was necessary to describe the structure and properties of the crystallinity of the Ta NPs under study. The peaks in the diffraction pattern for the XRD studies clearly depict the existence of diffractions from different crystallographic planes with Miller indices, (hkl) of the Ta NPs. Specifically, peaks corresponding to the (111), (200), and (220) planes are observed at positions with 2θ values of 38.571°, 55.714°, and 69.643°, respectively. These angles represent the diffraction angles where x-rays are scattered by the atomic planes of the tantalum crystal lattice. The (111) peak, observed at 2θ = 38.571°, is typically the most intense peak in the XRD pattern. This indicates that the (111) plane has the highest atomic packing density and is the most preferred orientation in the tantalum nanoparticle sample.

Table (1) Structural parameters for Ta NPs

2θ (deg)	FWHM (deg)	d_{hkl} (Å)	C.S. (nm)	Phase	(hkl)
38.571	0.700	2.3323	12.0	Ta	(111)
55.714	0.843	1.6485	10.7	Ta	(200)
69.643	0.851	1.3490	11.4	Ta	(220)

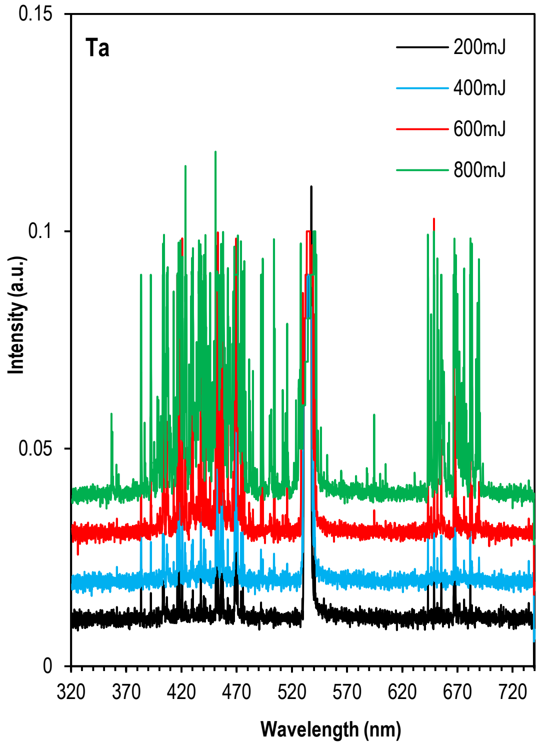

Fig. (2) Emission spectra of Ta target in distilled water produced using 532nm laser and different laser energies

The Zeta potential measurement was conducted using a Zeta potential analyzer, as depicted in Fig. (4). The Zeta potential technique provided valuable insights into the surface charge and stability of tantalum particles in the study. With measured Zeta potential values of 22.55mV for 1064nm and 24.17mV for 532nm laser wavelengths, the study demonstrated the stability of tantalum surfaces under experimental conditions. The stability of the particles in colloidal systems is influenced by different forces, including electrostatic repulsion and van der Waals forces, which can be represented quantitatively with respect to the zeta potential (Z.P.).

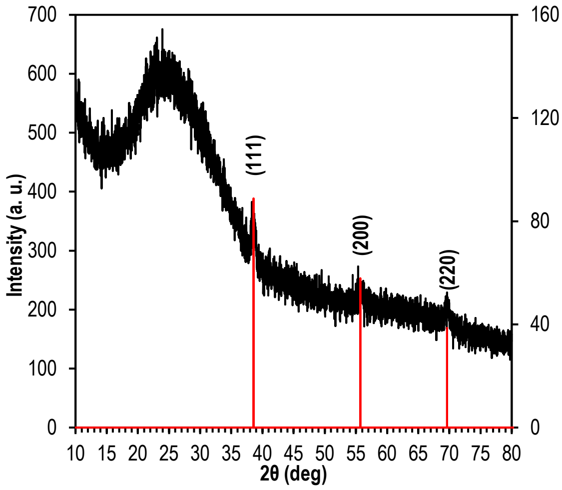

Fig. (3) XRD pattern of Ta NPs

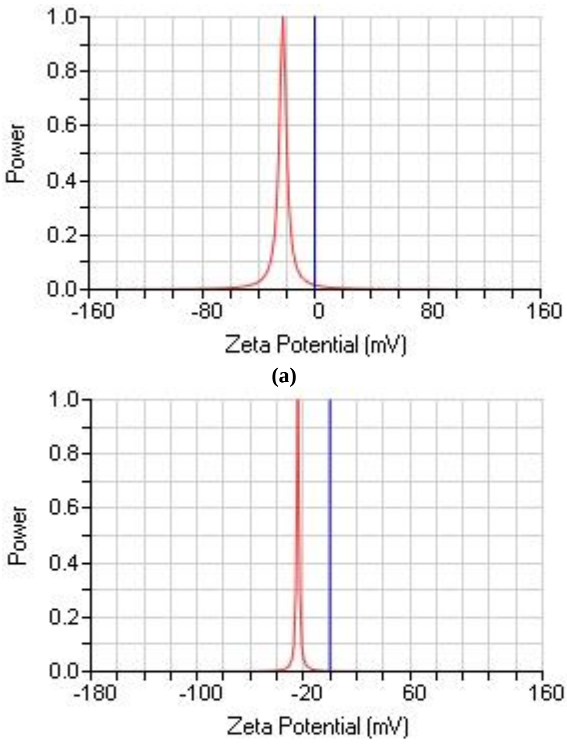

Fig. (4) Zeta potential curves for Ta (a) at 1064nm laser wavelength and (b) at 532nm laser wavelength

Through the Boltzmann plot technique, figures (5) and (6) provide detailed insights into the spectral analysis of tantalum particles induced by plasma under different laser conditions. The inverse relationship of photon energy to wavelength, coupled with particle expansion at higher energies, complicates the dynamics of laser-material interaction. In this work, simulations were done using two different laser wavelengths, 532 and 1064 nm, to ascertain the effects on the plasma properties of tantalum as the laser energies change.

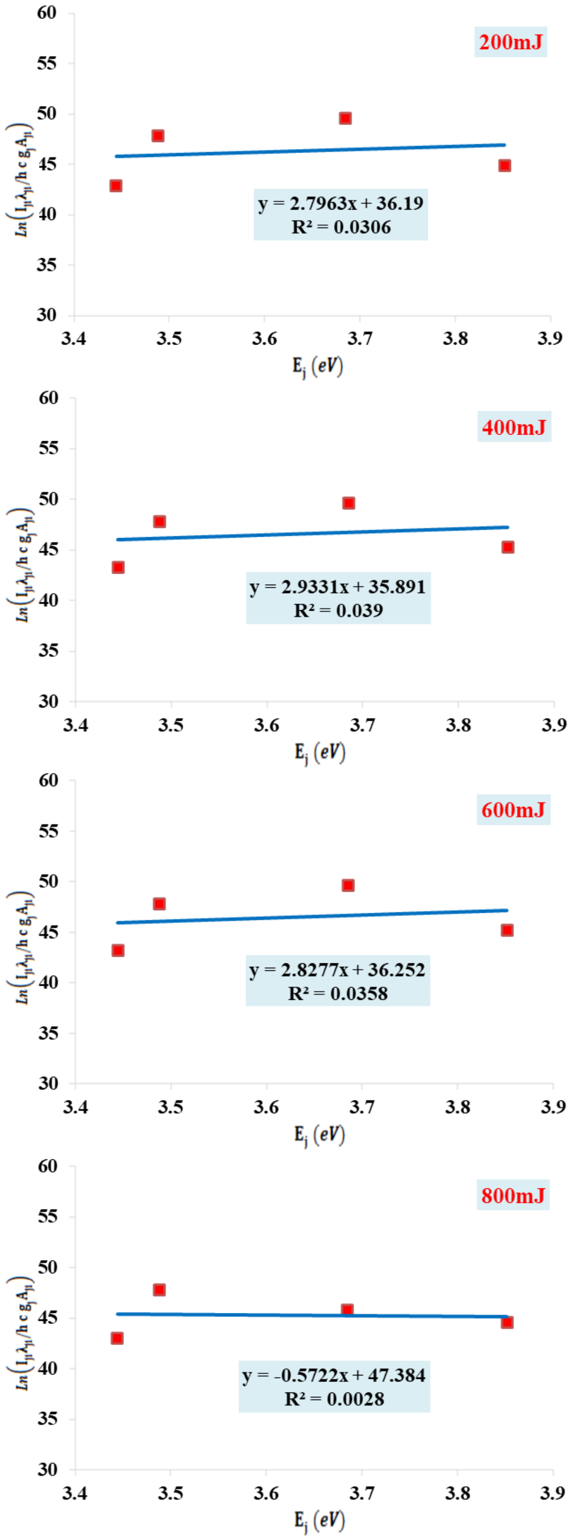

Fig. (5) Boltzmann diagrams of plasma induced with different laser energies for a Ta target using 1064nm laser

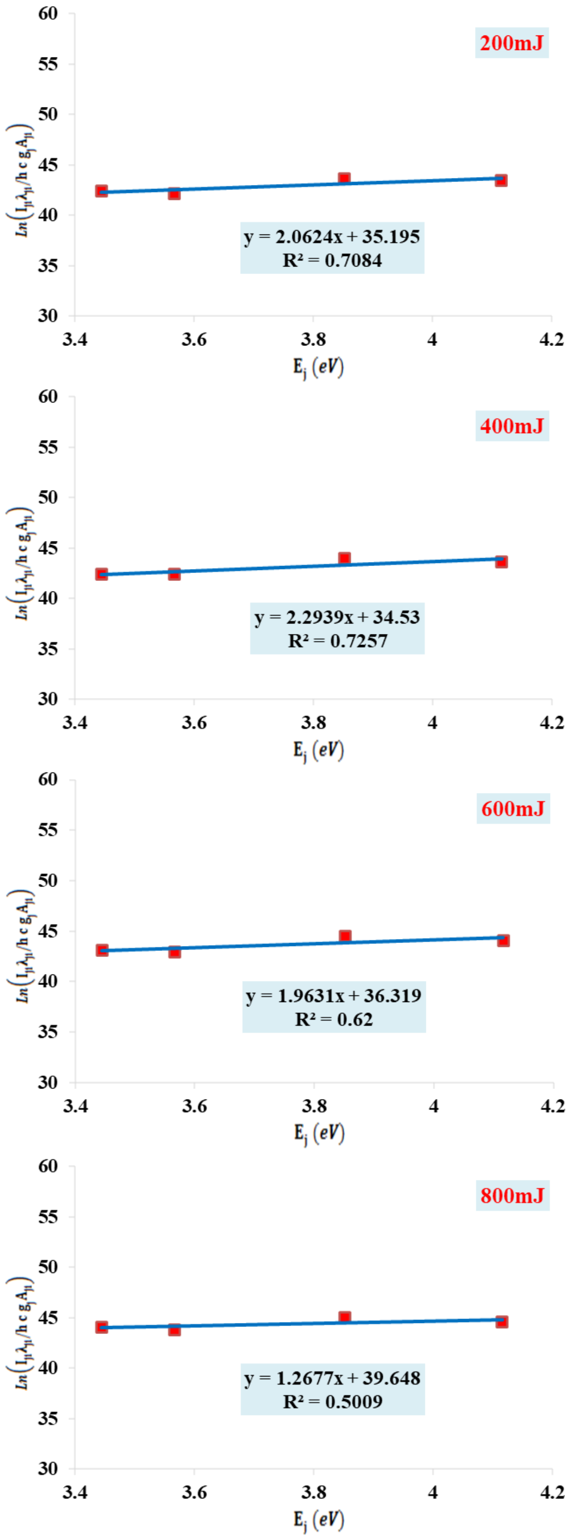

Fig. (6) Boltzmann diagrams of plasma induced with different laser energies for a Ta target using 532nm laser

Tables (2) and (3) present the values of electron temperature, electron density, Debye length, plasma frequency, and Debye number experimentally evaluated. All these parameters are very useful in understanding the behavior of plasma for different conditions of excitation. The tabulated results clearly bring out that T_e increases with a rise in the laser energies from 200 to 800mJ. This increase is attributed to the rise in energy transferred to electrons from the laser source during excitation. An increase in the electron temperatures boosts the possibility of ionization collisions, which then affects the behavior and characteristics of the resulting plasma. High average electron energy raises the possibility of ionization collisions, hence high electron density.

Table (2) Plasma parameters for Ta determined through the analysis of spectroscopy lines using a 1064 nm laser, considering various laser energies (E)

E (mJ)	T_e (eV)	n_e x10^{18} (cm^{-3})	ω_{pe} x10^{11} (rad/s)	λ_Dx10^{-6} (cm)	N_D
200	2.796	0.957	553.043	1.269	8239
400	2.933	1.137	602.679	1.193	8122
600	2.828	1.136	602.427	1.172	7692
800	0.572	0.7113	476.700	0.666	8850

Table (3) Plasma parameters for Ta determined through the analysis of spectroscopy lines using a 532 nm laser, considering various laser energies (E)

E (mJ)	T_e (eV)	n_e x10^{18} (cm^{-3})	ω_{pe} x10^{11} (rad/s)	λ_Dx10^{-6} (cm)	N_D
200	2.062	2.253	848.339	0.711	3402
400	2.294	1.903	779.641	0.816	4342
600	1.963	2.112	821.394	0.716	3263
800	1.268	2.184	835.212	0.566	1665

Plasma frequency depends mainly on the square root of n_e and therefore shows similar trends. On the other hand, the Debye length (λ_D) depends proportionally on $(T_e/n_e)^{1/2}$, while the Debye number (N_D) depends proportionally to ($T_e^{3/2}$ and $n_e^{1/2}$), and thus a high increase of n_e and a moderate increase in T_e make both λ_D and N_D to show significant increases. Figure (7) shows the electron temperature and electron density of the tantalum-induced plasma in distilled water by 532nm and 1064nm laser wavelengths.

4. Conclusion

Pulses from an Nd:YAG laser with two different wavelengths of 1064nm and 532nm were applied on tantalum surfaces showed very distinct effects on parameters. An exponential increase in electron temperature was observed from 2.79 to 2.83eV for Ta, while electron density decreased from 1.137×10^{18} to 0.711×10^{18} cm^{-3} as laser energy ramped up from 200 to 800mJ. Importantly, all calculated plasma parameters satisfied necessary conditions for plasma behavior. Notably, values of electron temperature and electron density were higher for tantalum under 1064nm irradiation compared to 532nm. These findings underscore the intricate relationship between laser energy, wavelength, and resulting plasma properties in tantalum ablation. The crystal structure of tantalum alters its surface characteristics, thereby influencing its reaction to laser irradiation and the subsequent formation of plasma. Additionally, the zeta potential, indicative of the surface charge of the plasma, plays a crucial role in determining the stability and behavior of the plasma generated.

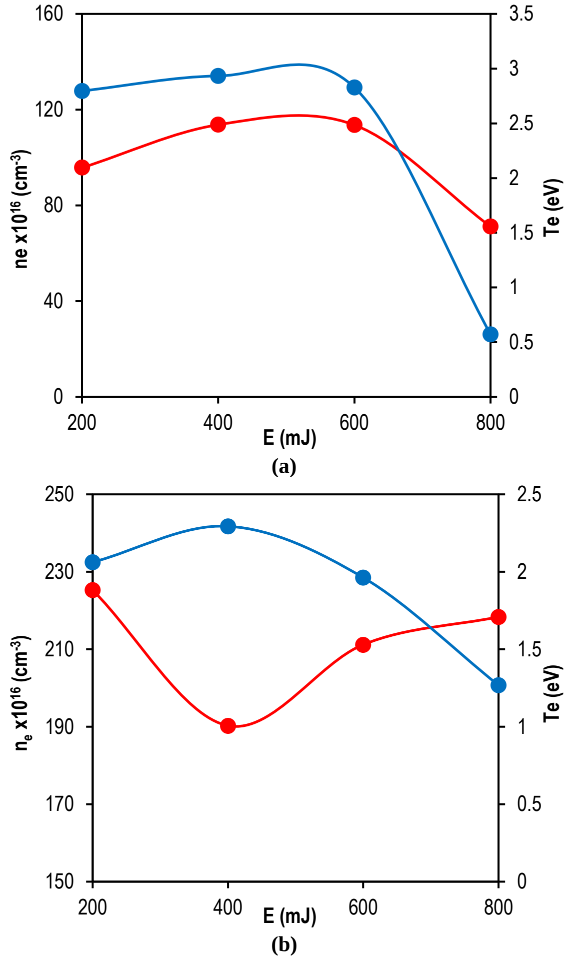

Fig. (7) Variation of electron temperature (T_e) and electron density (*n_e*) for Ta target using laser wavelength of (a) 1064nm, (b) 532nm

References

[1] J.C. Miller, **"Laser Ablation: Principles and Applications"**, *Springer Science & Business Media* (2013) pp. 11-14.

[2] J. Nogues, M.D. Baro and J. Sort, "Laser Ablation in Materials Science: From Mechanisms to Applications", *Prog. Mater. Sci.*, 52(3) (2007) 487-573.

[3] A.F. Mahood, "Emission Lines of Laser-Produced Plasmas of Metal Targets Using Optical Emission Spectroscopy", *Iraqi J. Mater.*, 2(1) (2023) 33-40.

[4] X. Mao and J. Gonzalez, "Fundamentals of Laser Ablation of Materials", *Rev. Mod. Phys.*, 85(1) (2013) 163-196.

[5] H. Sattari, N. Razmjou and M. Rezayi, "Laser Ablation and Its Applications in Nanotechnology", *J. Nanosci. Nanotech.*, 10(4) (2010) 2493-2503.

[6] T.E. Itina, S. Barcikowski and B.N. Chichkov, "Femtosecond Laser Ablation: Basics and Applications", *J. Appl. Phys.*, 106(5) (2009) article 051101.

[7] D. Liu, Z. Chen and H. Xu, "Plasma Plume Characteristics of Laser Ablation", *J. Appl. Phys.*, 89(3) (2001) 1374-1381.

[8] S. Maruo and H. Inoue, "Optical Trapping and Manipulation Using Laser Ablation", *Opt. Exp.*, 13(26) (2005) 10865-10870.

[9] A. Vogel, V. Altmann and A. Leipertz, "Mechanisms of Pulsed Laser Ablation of Biological Tissues", *Chem. Rev.*, 103(2) (2003) 577-644.

[10] R. Stoian and A. Rosenfeld, "Laser-Induced Plasmas in Analytical Spectroscopy", *Spectrochimica Acta B: Atom. Spectro.*, 57(7) (2002) 11043-11075.

[11] K. Du, Ja. Fabbri and Q. Gong, "Plasma Dynamics in Laser Ablation", *Phys. Rep.*, 503(1) (2011) 33-69.

[12] C.K. Gupta and A.K. Suri, **"Extractive Metallurgy of Niobium"**, CRC Press (1994), p. 27.

[13] A. Bogaerts and J.R. Brocaille, "Determination of Electron Temperatures in Low-Pressure Plasmas Using Optical Emission Spectroscopy: Application to Inductively Coupled Plasmas", *Spectrochimica Acta B: Atom. Spectro.*, 56(6) (2001) 947-958.

[14] H.J. Hassan, A.K. Abbas and I.M. Ibrahim, "Adding silver oxide on photoconductive characterizations of (Au-CeO_2) thin-film deposited on porous silicon p-type", *AIP Conf. Proc.*, 2834(1) (2023) 090006.

[15] S. Hübner, A. Piel and U. Czarnetzki, "High-Precision Measurements of Electron Temperatures in Nonequilibrium Low-Pressure Plasmas by Raman and Thomson Scattering", *Phys. Rev. Lett.*, 110(2) (2013) 025004.

[16] I. bin Selima, R. Fortier and A. El-Mahdi, "Laser-Based Measurements in Non-Equilibrium Plasmas", *Iraqi J. Mater.*, 3(3) (2023) 7-16.

[17] W. Zheng, X. Zhang and K. Yang, "Electron Temperature Measurement in Inductively Coupled Plasmas Using OES and TDLAS", *J. Anal. Atom. Spectrom.*, 31(4) (2016) 901-909.

[18] J.J. Mullen, E.G. Johansson and G. Ericsson, "Electron Temperature Measurements in a Magnetized Dusty Plasma", *Phys. Rev. E*, 94(3) (2016) 033206.

[19] N. Omenetto and P.J. Shull, "Electron Temperature Measurements in Laser-Produced Plasmas Using Balmer Line Emission", *Rev. Sci. Instrum.*, 63(10) (1992) 4586-4595.

[20] K. Pardnsar, “Secondary Electron Emission in Glow Discharge Plasmas”, *Iraqi J. Mater.*, 2(4) (2023) 167-174.
[21] I. I. Sobelman, "Atomic Spectra and Radiative Transitions," *Springer*, (1996) 64.
[22] C. J. Foot, "Atomic Physics," *Oxford University Press*, (2005) 132.
[23] M. N. Shneider, T. A. Pikuz, and I. Y. Skobelev, "Stark Broadening and Shift of Spectral Lines: Measurements and Applications in Laser-Produced Plasmas", *Journal of Quantitative Spectroscopy and Radiative Transfer*, 111(5), (2010) 817-830.
[24] H. R. Griem, "Spectral Line Broadening by Plasmas and the Inverse Problem", *Plasma Physics and Controlled Fusion*, 23(6), (1981) 689-703.
[25] D. R. Shklyar and A. P. Nagornyi, "Stark Broadening of Spectral Lines in Plasmas," *Springer*, (2001) 148.
[26] M. S. Dimitrijević and N. Konjević, "Stark Broadening of Spectral Lines by Plasmas," Springer, (2012) 97.
[27] W. L. Wiese, "Spectral Line Broadening by Plasmas," in "Advances in Atomic and Molecular Physics," *Academic Press*, (1967) 124.
[28] F. F. Chen, "Plasma Physics and Engineering," *CRC Press*, (2016)89.
[29] F. F. Chen, "Introduction to Plasma Physics and Controlled Fusion", *Springer*, (2006) 74.